Biochimica et Biophysica Acta, 307 (1973) 491–512

BBA 76336

THE STRUCTURE OF *ESCHERICHIA COLI* MEMBRANES STUDIED BY FLUORESCENCE MEASUREMENTS OF LIPID PHASE TRANSITIONS

HERMANN TRÄUBLE and PETER OVERATH

Max-Planck-Institut für Biophysikalische Chemie, D34 Göttingen-Nikolausberg, and Institut für Genetik der Universität zu Köln, D 5 Köln-41 (Germany)

(Received February 6th, 1973)

SUMMARY

Lipid phase transitions in *Escherichia coli* membranes and in dispersions of the extracted lipids were studied using the negatively charged fluorescence probe 1-anilinonaphthalene-8-sulfonate (ANS^-) and the hydrophobic fluorescence probe *N*-phenyl-1-naphthylamine (NPN). The fluorescence change, ΔI, at the phase transition approaches a limiting value $(\Delta I)_{lim}$ with increasing dye concentration. A comparison of the limiting values $(\Delta I)_{lim}^{NPN}$ obtained for membranes and the lipid standard allows us to estimate the lipid fraction, ρ, in the membrane that takes part in the phase transition ($\rho = 80\%$). The same procedure carried out with ANS^- yields a value of 42.5% for the lipid fraction that is accessible from the aqueous phase. These values, combined with published freeze–etching data for the particle density within the fracture plane of membranes are used to quantify the Davson–Danielli–Robertson–Benson–Singer membrane model which assumes a fluid lipid bilayer with "integral" proteins embedded in the lipid matrix and surface proteins attached to the lipid head groups. It appears that on the average one "integral" membrane protein is surrounded by about 600 lipid molecules and that about 130 of these molecules are closely coupled to the protein molecule, forming an halo in which the chain–chain interaction between the lipids is disturbed. About half of the bilayer surface is covered with proteins; part of these seem to be stacked.

INTRODUCTION

Lipid–lipid interaction is a well established phenomenon for a variety of biological membranes. This is directly demonstrated by the occurrence of lipid phase transitions (crystalline–liquid crystalline phase transition) in the membranes of *Mycoplasma laidlawii*[1–4], *Escherichia coli*[5–7] and mammalian membranes[8]. Phase transitions of this type rely on direct and cooperative interaction between the hydrocarbon chains of a large number of molecules as demonstrated by the occurrence of similar phase transitions in pure hydrocarbon materials[9–12]. Lipid phase transitions are virtually independent of whether the lipids exist as monolayers or bilayers[13,14]. However, recent X-ray investigations provide strong evidence for the presence of

Abbreviations: ANS^-, 1-anilinoaphthalene-8-sulfonate; NPN, *N*-phenyl-1-naphthylamine.

lipid bilayers in a number of plasma membranes[15–19]. However, these experiments do not allow the estimation of the fraction of phospholipids in bilayer form.

General principles for the arrangement of membrane proteins have not yet been established (*cf.* reviews by Stoeckenius and Engelman[20]; Hendler[21]; Singer[22]; Singer and Nicolson[23]; Blaurock[17]; Gitler[60]). There is evidence that some of the membrane proteins are bound rather firmly to the membrane lipids whereas others are held to the membrane only by weak interactions[24]. Singer[22] and Singer and Nicolson[23] have introduced the notations integral and peripheral proteins for these two classes of membrane proteins. This notation will also be used in the present paper.

A first attempt to describe the membrane structure quantitatively could be made if the following two parameters were known: (1) the fraction, ρ, of the lipids in bilayer form, and (2) the fraction of the lipid polar groups in contact with the water. In the present paper the fluorescence probes 1-anilinonaphthalene-8-sulfonate (ANS^-) and *N*-phenyl-1-naphthylamine (NPN) were used to estimate these parameters for the membrane of *E. coli*. Adsorption of these probes to membranes leads to an increase in the fluorescence intensity, I, and to a blue shift of the wavelength of maximum emission[25–27]. Since similar spectral changes are observed when the dyes are dissolved in media of low dielectric constant these probes are said to sense the polarity of their environment[28–30]. The dependence of the quantum yield, Q, and the wavelength of maximum emission of NPN on the solvent dielectric constant is shown in Fig. 1. For ANS^- a similar relationship has been established by Stryer[31].

Concerning the location of the dyes in the membranes there is good evidence that the negatively charged ANS^- binds to the membrane surface and orients with its sulfonic acid group in the aqueous phase[32–34]. The adsorption of ANS^- depends sensitively on surface charges and on the presence of counterions shielding these charges[27,35,36]. The neutral NPN, unlike ANS^-, is only sparingly soluble in water (deviations from Beer–Lamberts law are observed for concentrations larger than $5 \cdot 10^{-5}$ M). Therefore NPN is expected to penetrate into the hydrophobic core of the membrane. This view about the location of the adsorbed dyes is supported by the respective values of the quantum yield Q. In dispersions of dipalmitoyllecithin the quantum yield of the adsorbed NPN is $Q = 0.33 \pm 0.03$, corresponding to a solvent dielectric constant $\varepsilon \leqslant 10$, according to Fig. 1. The value for ANS^- is $Q = 0.16 \pm 0.04$, corresponding to a solvent dielectric constant $\varepsilon \approx 35$. Recent NMR studies by Colley and Metcalfe[37] support the view that ANS^- is located in the membrane–water interface, whereas NPN penetrates deeply into the membrane hydrocarbon region. Concerning the distribution of the incorporated NPN molecules in the plane of the membrane it was shown in recent ESR studies[38–40] that a fluid lipid matrix permits rapid lateral diffusion of lipid molecules and other lipid-soluble molecules. Therefore we may firmly assume that the adsorbed NPN molecules are distributed randomly in the plane of the lipid matrix.

The main difficulty in the application of fluorescent dyes such as ANS^- to membranes is their tendency to interact almost equally well with membrane proteins and lipids (*cf.* Radda[28–30]). In order to separate these two effects one can study a membrane property which is determined exclusively by the membrane lipids and which is sensitively reflected in the fluorescent or adsorption properties of the applied dye. Lipid phase transitions are ideally suited for this purpose. As described elsewhere[7], the fluorescent dyes ANS^- and NPN are useful indicators of phase transi-

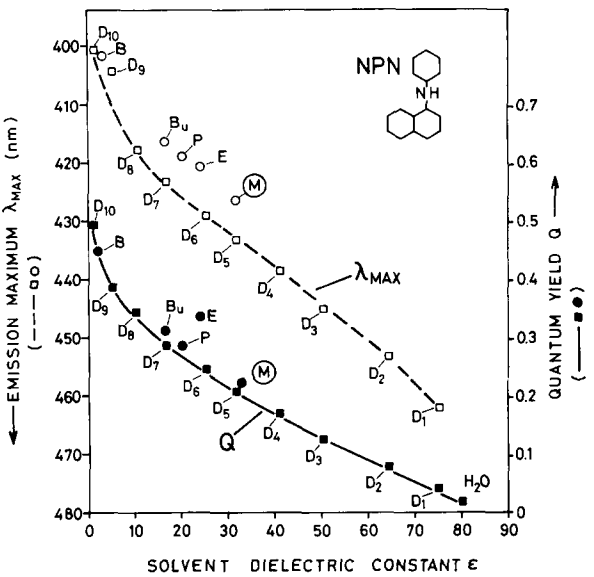

Fig. 1. *N*-Phenyl-1-naphthylamine (NPN); quantum yield, Q, and wavelength of maximum emission, λ_{max}, as a function of the dielectric constant ε of the solvent. The symbols D_1 to D_{10} denote dioxane–water mixtures containing between 10 to 100% dioxane (v/v). The corresponding values of ε were taken from the paper by Turner and Brand[59]. M, methanol; E, ethanol; P, *n*-propanol; Bu, n-butanol; B, benzene. Wavelength of excitation: 340 nm. The *Q* values were determined relative to the known value in methanol $Q=0.22$ (Radda[29]).

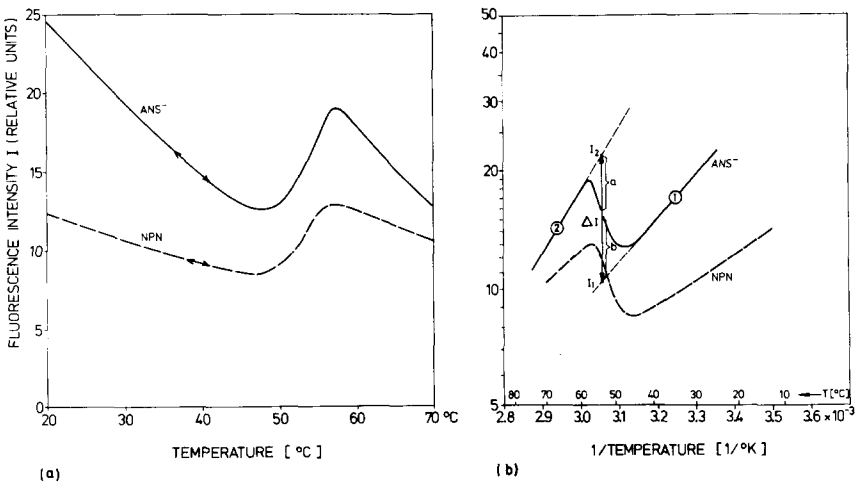

Fig. 2. Response of the fluorescence intensities *I* of ANS⁻ and NPN to the thermal phase transition of distearoyllecithin dispersions (2.5×10^{-4} M lecithin). (a) *I versus T*; (b) log *I versus* $1/T$, straight lines (with different slopes) are obtained for the two states below (1) and above (2) the phase transition. ΔI is defined as the vertical difference (I_2–I_1) between the extrapolated lines at a temperature T_t where the measured curve bisects the difference (I_2–I_1) (num a = num b). ANS⁻: excitation at $\lambda=360$ nm, emission at $\lambda=480$ nm; $5.3\cdot10^{-5}$ M ANS⁻, $4.2\cdot10^{-2}$ M NaCl. NPN: excitation at $\lambda=360$ nm, emission at $\lambda=425$ nm; $1\cdot10^{-5}$ M NPN. The rate of temperature change was 1 °C/min. The fluorescence intensities of ANS⁻ and NPN alone in water are virtually independent on temperature in the investigated range.

tions in dispersions of synthetic lipids or intact membranes. An abrupt change in the fluorescence intensities, I, of ANS^- and NPN is observed in the temperature range of the lipid phase transition (*cf.* Fig. 2). The fluorescence change ΔI (for the exact definition of ΔI see legend to Fig. 2b and Appendix) at the phase transition is a function of the total dye concentration, c: ΔI increases sharply with increasing c for small dye concentrations and approaches a limiting value $(\Delta I)_{lim}$ for higher concentrations. Thus the dependence of ΔI on c resembles a titration curve (*cf.* Appendix, Eqns A7 and A9).

As shown in the Appendix the value of $(\Delta I)_{lim}$ can be used as a measure of that fraction of the membrane lipids which participates in the lipid phase transition, and, at the same time, is accessible to the fluorescent probe. In the case of ANS^- (surface probe), only that fraction of the lipid layer contributes to $(\Delta I)_{lim}^{ANS^-}$ which is accessible from the aqueous phase, whereas in the case of NPN (bulk probe) the value of $(\Delta I)_{lim}^{NPN}$ is a measure of the total lipid fraction participating in the lipid phase transition.

Values of the respective lipid fractions in the intact membrane can be determined by a comparison with corresponding measurements on dispersions of the isolated membrane lipids. This procedure then allows to estimate: (a) from the value $(\Delta I)_{lim}^{NPN}$ the fraction, ρ, of the membrane lipids participating in the phase transition, and (b) from the value $(\Delta I)_{lim}^{ANS^-}$ the fraction, μ, of these lipids accessible from the aqueous phase.

MATERIALS AND METHODS

Membranes

The fatty acid auxotroph *E. coli* strain K 1062 was grown at 39 °C in the presence of *trans*-Δ^9-octadecenoic acid (*trans*-18:1, elaidic acid) as described elsewhere[7]. Under these conditions about 70% of the fatty acids of the membrane lipids are elaidic acid. Membranes were isolated according to the method of Kaback[41]. About 90% of the weight of this preparation were plasma membranes, the rest were fragments of the outer membrane (*cf.* Overath and Träuble[7]). The stock membrane suspension contained 22 mg protein and 10.2 mg phospholipid per ml, corresponding to a protein–lipid ratio of 2.16.

Phospholipids

The membrane lipids used in the present study were extracted by the method of Ames[42] with chloroform–methanol. The extract contained 82 mole% phosphatidylethanolamine, 11.1 mole% cardiolipin and 7.2 mole% phosphatidylglycerol. The fatty acid composition of the extracted lipids and the membranes (values in parentheses) were*: 12:0 = 1.6 (4.1); 14:0 = 14.0 (8.1); 16.0 = 13.5 (9.7); 16.1 = 2.6 (< 1); *trans*-Δ^9-18:1 = 68.3 (78). The average molecular weight of the lipids was 777. The transition temperatures of the individual components, of the total lipids and the intact membranes were studied in a separate paper (Overath and Träuble[7]).

* The number before the colon gives the number of carbon atoms, the number after the colon gives the number of double bonds. Subscript to Δ gives the position of ethylenic bond.

Lipid and membrane dispersions

Lipids were dispersed ultrasonically at 42 °C under nitrogen. Optically clear solutions were obtained within 1–3 min of sonication (60 W). The stock dispersions were diluted with buffer and/or salt solutions to a final lipid concentration of $5 \cdot 10^{-5}$ M. Membranes were sonicated at 25 °C for about 30 s and diluted to a lipid content of $5 \cdot 10^{-5}$ M yielding optically clear solutions.

Fluorescence probes

ANS^- (1-anilinonaphthalene-8-sulfonate) was purchased as ammonium salt (mol. wt = 318) from Pierce Chemicals; NPN (N-phenyl-1-naphthylamine, mol. wt = 219) was obtained from Kodak Co. Stock solutions of ANS^- in water ($1 \cdot 10^{-3}$–$5 \cdot 10^{-3}$) and NPN in methanol (10^{-3}–10^{-5} M) were prepared daily and stored in the dark. A methanol content below 3% (v/v) did not influence the lipid transition.

Fluorescence measurements

The fluorescence probes were added to 3-ml aliquots of the dispersions; these solutions were held for 30 min at 45–50 °C prior to the measurements. Several temperature scans, $I(T)$, of the fluorescence intensity, I, were recorded at decreasing and increasing temperature at a maximum rate of temperature change of 1 °C/min using an Aminco Bowman spectrofluorimeter. If not stated otherwise, the reproduced curves were measured at increasing temperature; before this at least one temperature scan was measured at decreasing temperature. The fluorescence signals were corrected for light scattering and inner filter effects; the latter correction is by far the most important because the excitation wavelengths of 360 nm for ANS^- and 340 nm for NPN correspond to absorption maxima. Correction curves were established by measuring the fluorescence intensity I of the probes in water as a function of the probe concentration. An exactly linear relationship between $\log(I/c)$ and c (c = dye concentration) was obtained for ANS^- over the whole concentration range; for NPN, deviations from a linear relation were observed for $c \geqslant 10^{-4}$ M due to the onset of aggregation of the dye in water.

Fluorescence standards were used to maintain constant instrumental conditions within each group of experiments (*cf.* Results). For each group of experiments the results are given in the same relative ordinate scale. Under the instrumental conditions used (1 cm × 1 cm cuvette, 2 mm slits) a reference solution containing $2.4 \cdot 10^{-6}$ M ANS^- in ethanol gave a fluorescence intensity (uncorrected) of 100 units at 25 °C if excited at 360 nm and measured at 480 nm.

Quantum yield Q

The quantum yields of the adsorbed probes were determined relative to the known quantum yields in ethanol ($Q = 0.37$ for ANS^- (Stryer[31])) and methanol ($Q = 0.22$ for NPN (Radda[29])) by plotting the reciprocal values of integrated spectra *versus* the reciprocal nominal lipid concentrations. The spectra were corrected for inner filter and light scattering effects (based on absorbance measurements). The reciprocal plots were then extrapolated to infinite lipid concentration.

RESULTS

The experiments were performed in two groups: In Group A increasing amounts of ANS^- were added (1) to dispersions of the extracted lipids and (2) to

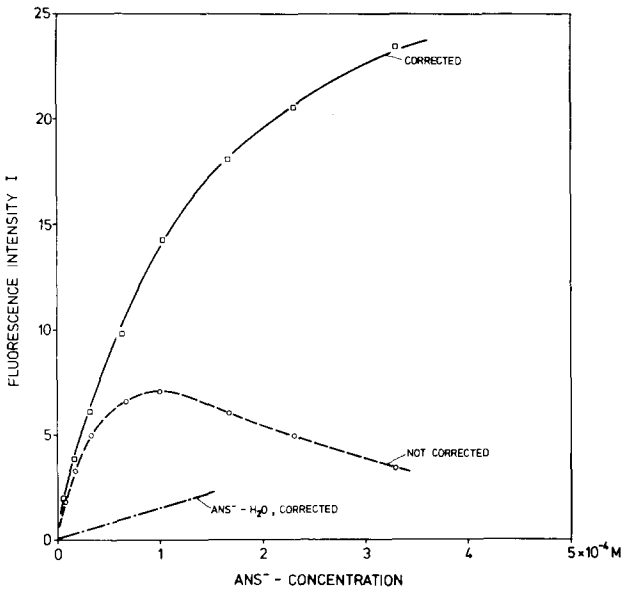

Fig. 3. Fluorescence intensity I of ANS$^-$ as a function of the ANS$^-$ concentration in dispersions of the extracted membrane lipids. This curve was measured at 45 °C prior to the temperature scans shown in Fig. 4. $5 \cdot 10^{-5}$ M lipid, 1 M NaCl. Wavelengths of excitation and emission: 360 nm and 480 nm. (——): Curve corrected for inner filter effects; fluorescence intensity of free ANS$^-$ not subtracted.

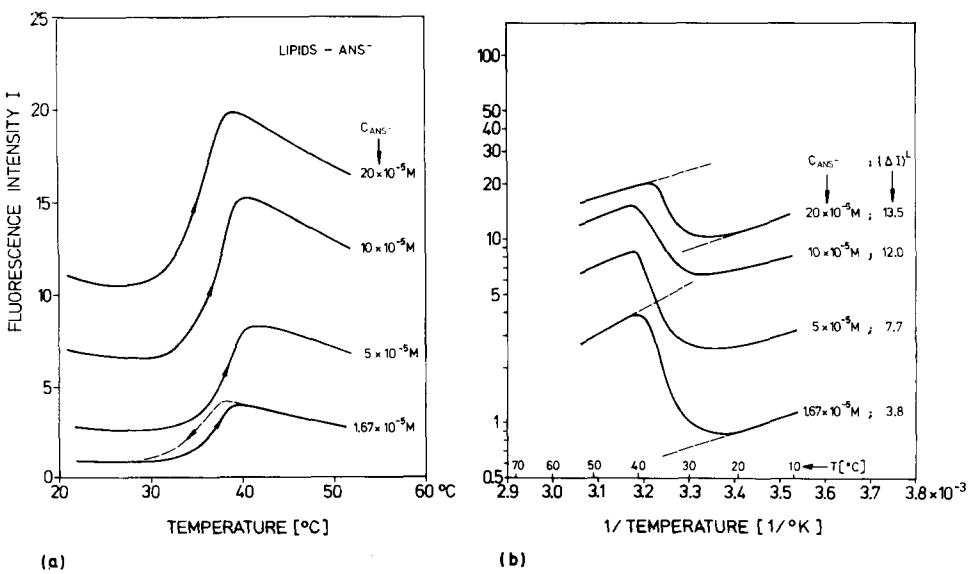

Fig. 4. Temperature scans of the ANS$^-$ fluorescence intensity, I, for different concentrations of ANS$^-$ in dispersions of membrane lipids (corrected for inner filter effects). $5 \cdot 10^{-5}$ M lipid, 1 M NaCl; excitation at 360 nm, emission at 480 nm. ANS$^-$ was added at 45 °C; the solutions were equilibrated for 30 min at 45 °C; then the temperature was reduced to 20 °C and raised again. The values of ΔI were determined from Fig. 4b.

membrane preparations. For each ANS^- concentration several temperature scans $I(T)$ were recorded between 20 °C and 55 °C starting at 55 °C. In Group B analogous experiments were performed using NPN as fluorescent probe.

Group A: phase transitions using ANS^- as a probe

(1) Lipid dispersions ($5 \cdot 10^{-5}$ M lipid, 1 M NaCl, neutral pH). Fig. 3 shows the binding of ANS^- to the extracted membrane lipids at 45 °C as measured by the fluorescence intensity. The quantum yield of the adsorbed dye is $Q = 0.015 \pm 0.002$ at 25 °C and $Q = 0.025 \pm 0.005$ at 45 °C. A series of temperature scans $I(T)$ measured at increasing temperature for different ANS^- concentrations is shown in Fig. 4a. For the lowest ANS^- concentration a curve recorded at decreasing temperature is also shown (– – – –) in order to demonstrate the degree of hysteresis observed in these experiments. This phenomenon will, however, not concern us here because the change in fluorescence intensity at the phase transition, ΔI, is the same for increasing and decreasing temperature. As seen in Fig. 4a the value of ΔI approaches a limiting value with increasing ANS^- concentration. In Fig. 4b the same curves

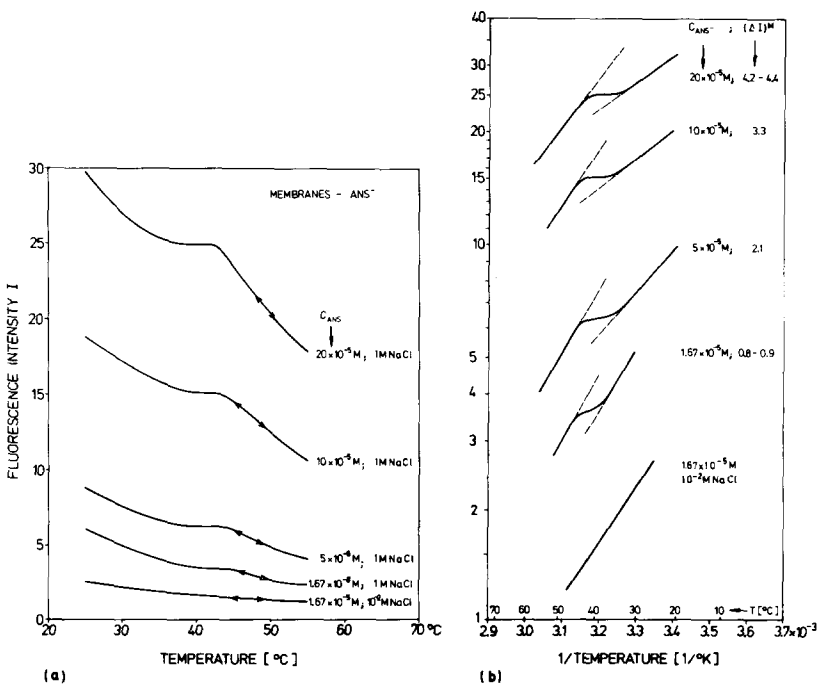

Fig. 5. Temperature scans of the ANS^- fluorescence intensity for different concentrations of ANS^- in membrane dispersions (corrected for inner filter effects). The membrane concentration was equivalent to $5 \cdot 10^{-5}$ M lipid. With exception of the lower curve (10^{-2} M NaCl) all measurements were made at 1 M NaCl. Excitation at 360 nm, emission at 480 nm. Ordinate scale and experimental conditions as in Fig. 4. In the *I versus T* plot (a) the lipid phase transition is indicated by a shoulder in the falling temperature characteristic. In the log *I versus* $1/T$ plot (b) the phase transition appears as a kink between two straight lines. For low ANS^- and low salt concentration the lipid effect is absent. The higher slope of the straight lines in Fig. 5b compared to Fig. 4b is due to ANS^-–protein binding. The decrease in slope with increasing ANS^- concentration indicates a relative increase of the ANS^-–lipid interaction.

are shown in a log I *versus* $1/T$ diagram. The values of $(\Delta I)^{L}$ (L for lipids) determined from this diagram are plotted in Fig. 6a as a function of the nominal ANS^- concentration, c_{ANS^-}. A reciprocal plot of $1/\Delta I$ *versus* $1/c_{ANS^-}$ gives a straight line (Fig. 6b). The intercept of this line with the zero ordinate determines a limiting value $(\Delta I)_{lim}^{L,ANS^-} = 16.7 \pm 1$.

(*2*) *Membrane dispersions* ($5 \cdot 10^{-5}$ *M lipid, 1 M NaCl, neutral pH*). The results of analogous experiments with membrane preparations are shown in Fig. 5. Virtually no hysteresis was observed in these experiments. In contrast to the lipid dispersions (Fig. 4a) the characteristic feature of these curves is a rather rapid decrease of the fluorescence intensity with increasing temperature. Comparison with Fig. 4a suggests that this behavior is due to the interaction of ANS^- with membrane proteins. With increasing ANS^- concentration a shoulder appears in these curves in about the same temperature range in which the isolated lipids show a phase transition. This effect is seen more clearly for higher ANS^- and/or salt concentrations. This may indicate that ANS^- has a higher affinity to the proteins than to the negatively charged membrane lipids (salt effect!) and that with increasing ANS^- concentration the protein binding sites are saturated earlier.*

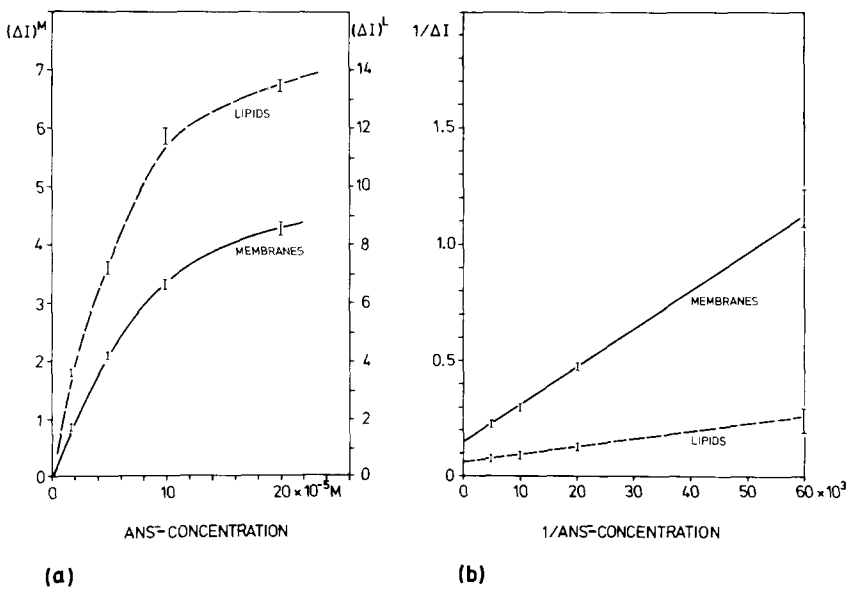

Fig. 6. Fluorescence amplitude ΔI at the phase transition for membranes $(\Delta I)^{M}$ and lipids $(\Delta I)^{L}$ as a function of the ANS^- concentration, c_{ANS^-}. (a) ΔI *versus* c_{ANS^-}; the left hand scale is for membranes, the right hand scale for lipids. (b) Reciprocal plot of $1/\Delta I$ *versus* $1/c_{ANS^-}$. The intercept with the zero ordinate yields for the limiting values $(\Delta I)_{lim}^{L,ANS^-} = 16.7 \pm 1$ and $(\Delta I)_{lim}^{M,ANS} = 7.1 \pm 0.5$.

* The detailed analysis of this point would require the knowledge of the respective numbers of binding sites, binding constants and quantum yields. Recent life time measurements of ANS^- adsorbed to red blood cells (Fortes[43]) indicate that ANS^- bound to proteins has a much higher quantum yield ($Q \approx 1$) than ANS^- interacting with lipids. In accordance with this, the emission spectra of ANS^- added to *E. coli* membranes exhibit besides the maximum at about 495 nm (characteristic for the ANS^-–lipid interaction) a shoulder at about 475 nm indicative of the ANS^-–protein interaction. This shoulder is seen most clearly at low ANS^- concentration.

The effect of the lipid phase transition is seen more clearly if log I is plotted *versus* $1/T$ (Fig. 5b)*. The values of $(\Delta I)^{M,ANS^-}$ obtained from these curves are plotted in Fig. 6 in the same way as before. Again a fairly straight line is obtained in a reciprocal plot of $1/\Delta I$ *versus* $1/c_{ANS^-}$. From the intercept of this line with the zero ordinate we obtain $(\Delta I)^{M,ANS^-}_{lim} = 7.1 \pm 0.5$.

Using the value $(\Delta I)^{L,ANS^-}_{lim} = 16.7$ as standard for the state in which all lipids participate in the phase transition and are accessible to ANS^- we arrive at a value of $42.5 \pm 5\%$** for the fraction of the total membrane lipids which (a) participates in the lipid phase transition and which, at the same time, (b) can adsorb ANS^- from the water. This demonstrates that a considerable part of the membrane lipids is directly accessible from the aqueous phase. A membrane model postulating continuous layers of proteins on both sides of the membrane is not compatible with this result.

In the following section we estimate the fraction ρ of the membrane lipids participating in the lipid phase transition.

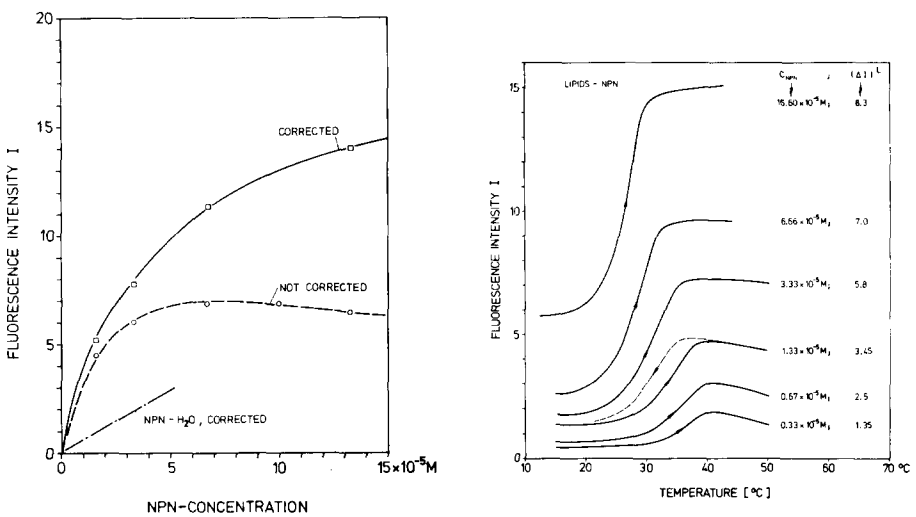

Fig. 7. Binding of NPN to membrane lipids at 45 °C as measured by the increase in fluorescence intensity; $5 \cdot 10^{-5}$ M lipid, 0.25 M NaCl. Excitation at 340 nm, emission at 480 nm; (——): corrected for inner filter effects; fluorescence of NPN in water not subtracted. This curve was measured prior to the temperature scans $I(T)$ shown in Fig. 8.

Fig. 8. Temperature scans of the fluorescence intensity I for different concentrations of NPN in lipid dispersions; (340 nm, 480 nm, corrected for inner filter effects, $5 \cdot 10^{-5}$ M lipid, 0.25 M NaCl). NPN was added at 50 °C; the solutions were equilibrated for 30 min, then the temperature was lowered slowly to 15 °C. The fluorescence change at increasing temperature is shown in the figure. Ordinate scale and instrumentation as in Fig. 7.

* The correlation between the fluorescence change, ΔI, and the lipid phase transition is demonstrated in a separate paper (Overath and Träuble[7]) for membranes with different lipid composition.

** The given numbers for the uncertainty denote extreme deviations; the values for the standard deviations are much smaller.

Group B: Phase transitions using NPN as a probe

(1) Lipid dispersions ($5 \cdot 10^{-5}$ M lipid, 0.25 M NaCl, neutral pH). Fig. 7 illustrates the binding of NPN to membrane lipids at 45 °C as measured by the increase in fluorescence intensity. The quantum yield Q of the adsorbed dye is $Q=0.375$ as compared with $Q=0.02$ for NPN in water. Temperature scans, $I(T)$, measured at different NPN concentrations are shown in Fig. 8. For an intermediate concentration two curves are shown, measured at decreasing and increasing temperature, to demonstrate the degree of hysteresis in these measurements. Again, the fluorescence change at the phase transition, ΔI, is virtually the same for both curves. The values of $(\Delta I)^{L,NPN}$ determined from these measurements are shown in Fig. 9a as a function

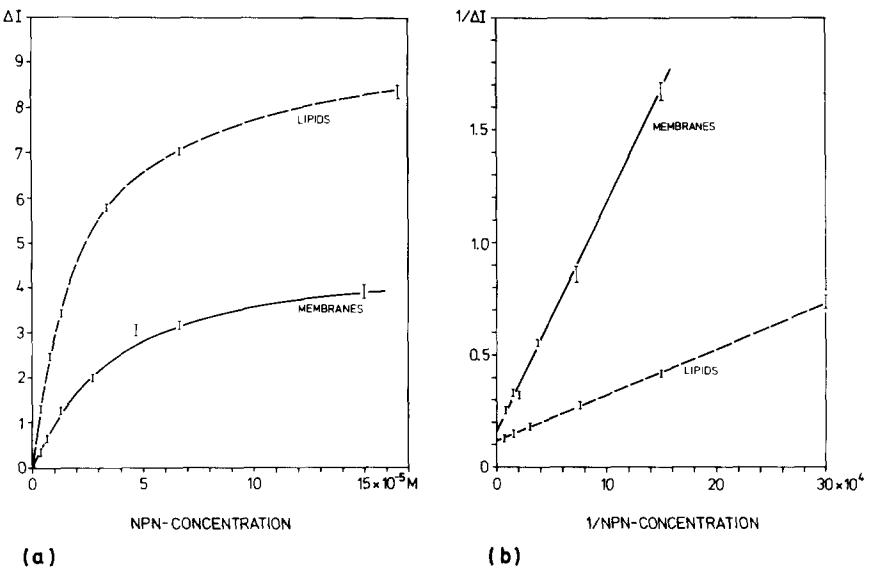

Fig. 9. Fluorescence amplitude ΔI at the phase transition for lipids and membranes as a function of the NPN concentration. (a) ΔI *versus* c_{NPN}. (b) Reciprocal plot of $1/\Delta I$ *versus* $1/c_{NPN}$. The intercepts of the straight lines with the zero ordinate determine the limiting values $(\Delta I)_{lim}^{L,NPN} = 8.35 \pm 0.2$ and $(\Delta I)_{lim}^{M,NPN} = 6.65 \pm 0.4$.

of the NPN concentration and in Fig. 9b in a reciprocal plot ($1/\Delta I$ *versus* $1/c_{NPN}$). As in the case of ANS^- the amplitude ΔI saturates with increasing dye concentration and the limiting value $(\Delta I)_{lim}^{L,NPN}$ can be determined from the intercept of the straight line in Fig. 9b with the zero ordinate as $(\Delta I)_{lim}^{L,NPN} = 8.35 \pm 0.2$. As seen in Fig. 8, at high NPN concentrations the transition temperature, T_t, is lower indicating that the incorporation of large amounts of NPN into the lipid structure "fluidizes" the lipid matrix. According to Fig. 9b this does, however, not affect the saturation behaviour of $(\Delta I)^{L,NPN}$ with increasing NPN concentration.

(2) Membrane dispersions ($5 \cdot 10^{-5}$ M lipid, 0.25 M NaCl, neutral pH). The binding of NPN to membranes was measured at 45 °C (*cf.* Fig. 10). The quantum yield of the adsorbed dye ($Q=0.375$) is exactly the same as for lipid dispersions. Using this value, the corrected binding curve in Fig. 10 (after subtraction of the fluorescence intensity of NPN in water) was converted into a c_L/c_{NPN}^* *versus* $1/c_{NPN}$

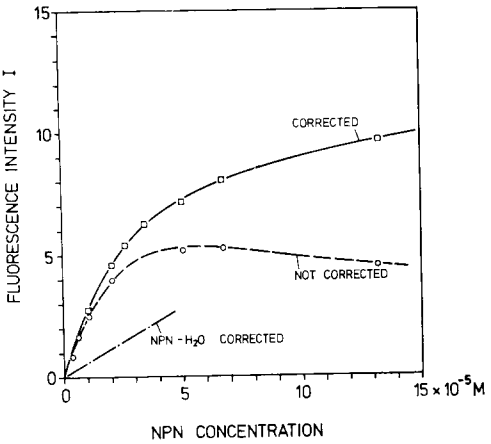

Fig. 10. Binding of NPN to membranes at 45 °C as measured by the fluorescence increase; (340 nm, 480 nm); (———): corrected for inner filter effects. The membrane concentration was equivalent to $5 \cdot 10^{-5}$ M lipid; 0.25 M NaCl. This curve was measured prior to the temperature scans shown in Fig. 11.

diagram (c_L = lipid concentration, c^*_{NPN} = concentration of the adsorbed NPN, c_{NPN} = nominal NPN concentration). From this plot we obtain for the equilibrium dissociation constant $K_D = 2 \cdot 10^{-4}$ M; and a value of 9 is estimated for the minimum number of lipid molecules providing one binding site for NPN.

The equality of the quantum yields of NPN bound to membranes and to lipids suggests that NPN, unlike ANS^-, does not strongly interact with the membrane proteins. This is also inferred from the similarity of the temperature scans $I(T)$ for membranes and lipids (compare Figs 11 and 8). The values of $(\Delta I)^{M,NPN}$ determined from the curves in Fig. 11 are shown in Fig. 9a in a linear plot (ΔI *versus* c_{NPN}) and

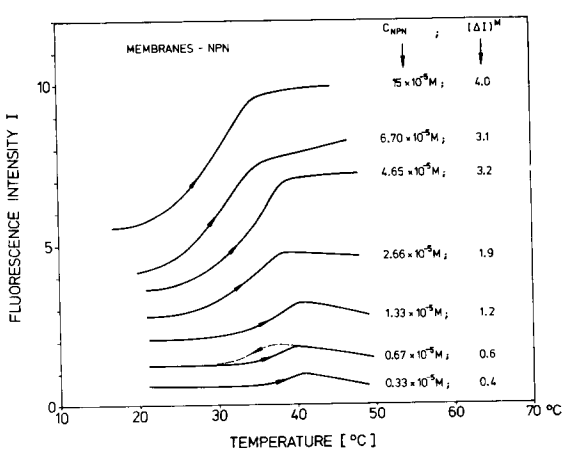

Fig. 11. Temperature scans of the fluorescence intensity I of NPN for different concentrations of NPN in membrane dispersions (340 nm, 480 nm). Corrected for inner filter effects. The membrane concentration was equivalent to $5 \cdot 10^{-5}$ M lipid; 0.25 M NaCl. NPN was added at about 50 °C, the temperature was slowly reduced to about 20 °C. The figure shows the fluorescence intensity at increasing temperature. Ordinate scale and instrumentation as in Figs 7, 8, 10.

in Fig. 9b in a reciprocal plot ($1/\Delta I$ *versus* $1/c_{NPN}$) together with the corresponding results for the lipids. From Fig. 9b one determines $(\Delta I)_{lim}^{M,NPN} = 6.65 \pm 0.4$.

Taking the value for the lipids, $(\Delta I)_{lim}^{L,NPN} = 8.35 \pm 0.2$, as a standard we arrive at $\rho = (80 \pm 6)\%$ for the fraction of the membrane lipids participating in the lipid phase transition. The rest of the lipids ($\rho' = 20\%$) must be present in a state in which the interaction between the lipid hydrocarbon chains is disturbed. It will be assumed below that these lipids are coupled to "integral" membrane proteins. According to the experiments of Group A a fraction of 42.5% of the total membrane lipids is at the same time (a) accessible to ANS^- and (b) participates in the lipid phase transition. Thus a fraction $\mu = 53\%$ of the lipids participating in the phase transition (fraction ρ) is accessible to ANS^- from the aqueous solution.

CRITICISM AND CONTROL EXPERIMENTS

The following objections may be raised against our experiments:

(1) The binding of the negatively charged ANS^- depends sensitively on fixed and adsorbed surface charges (*cf.* Gomperts *et al.*[35]; Träuble[36]). Therefore titration experiments with ANS^- yield "true" saturation values only if the ionic strength is sufficiently high to shield the surface charges.

(2) Lipid and membrane dispersions may contain closed vesicles that are impermeable to ANS^-. This would reduce the membrane surface to which ANS^- can adsorb; consequently the above value of μ would be subject to considerable uncertainty because the fraction of closed vesicles in our preparations is not known.

In order to check points 1 and 2 the experiments of Group A were repeated at different salt concentrations ((a) 0.1 M NaCl, (b) 1 M NaCl and (c) 0.1 M $CaCl_2$) and with the difference that the ANS^- was added prior to the sonication. The latter procedure ensures that the ANS^- is present also on the inside of closed vesicles (*cf.* Bergelson *et al.*[44]). The $(\Delta I)_{lim}$ values of all these experiments were practically identical, and differed from the results of the previous experiments by not more than 4%. Therefore, if closed vesicles were present in the previous experiments then the ANS^- had penetrated into these vesicles during the sample preparation (addition of ANS^- after the sonication and equilibration of the samples at 45 °C for 30 min).

(3) The lipid phase transition may induce structural changes in membrane proteins which in turn may lead to changes in the ANS^- fluorescence intensity (protein contribution to ΔI). This effect can be important especially in the case of ANS^- which interacts strongly with membrane proteins*. There is, however, evidence that the observed fluorescence change, ΔI, is a true lipid effect. According to Fig. 5a the lipid phase transition is indicated only by a small shoulder in the temperature dependence of the ANS^- fluorescence intensity. For very low ANS^- and/or salt concentrations (binding of ANS^- predominantly to proteins; *cf.* legend to Fig. 5) this shoulder is completely absent as indicated by the lower tracings in Fig. 5. This rules out the possibility that structural changes in the membrane proteins lead to abrupt changes in the ANS^- fluorescence intensity in the range of the lipid phase transition.

* In contrast, NPN does not, or only weakly interact with membrane proteins. This may be inferred from a comparison of Figs 8 and 11 and from the exact agreement of the quantum yield of NPN in lipid and membrane suspensions.

(4) X-ray studies by Chapman *et al.*[45] have shown that the molecular area of the lipid molecules changes by about 20% during the lipid phase transition. Therefore some of the lipid molecules that are covered with surface proteins in the state $T<T_t$ may become accessible to ANS^- for $T>T_t$. In other words, the number of free lipid molecules (not covered by proteins) may be larger for $T>T_t$. Denoting the concentrations of the free lipid molecules in the two states $T<T_t$ and $T>T_t$ by $c_{L,1}$ and $c_{L,2}$ respectively ($c_{L,2}=c_{L,1}+\Delta c_L$) we obtain, for the limiting value $(\Delta I)_{lim}$, the following expression (*cf.* Appendix):

$$(\Delta I)_{\text{lim}}^{\text{M,ANS}^-} = c_{L,1}(Q_2^*\ n_2 - Q_1^*\ n_1) + Q_2^*\ n_2 \Delta c_L$$

In this case ($\Delta c_L \neq 0$) the value of μ estimated from $(\Delta I)_{\text{lim}}^{\text{M, ANS}^-}$ must be considered as an upper limit. The magnitude of this effect can be estimated as follows. Our measurements indicate ($\mu=53\%$) that about half of the bilayer area is covered with proteins. Assuming a 20% change in the lipid molecular area at T_t would mean that our value of μ is too high by about 10%.

(5) The ultrasonic irradiation of the membranes (30 s at room temperature) may release proteins from the membrane. Control experiments showed that the applied sonication released not more than 5% of the membrane proteins, as judged by a protein determination in the supernatant after 1 h centrifugation at $100000\times g$. This result is in good accordance with similar findings by Kamat *et al.*[46] for erythrocyte membranes. The effect of a reduced protein content in the membrane preparations would be that the area of "free" lipids (μ) appears as too large.

(6) The ANS^- may penetrate into the space between the surface proteins and the underlying lipid bilayer. This does not make any difference if the value of μ is interpreted strictly as the "accessible" part of the lipid bilayer. If, however, μ is considered as the area of the bilayer not covered with proteins then our value of $\mu=53\%$ must be regarded as an upper limit.

(7) The adsorbed ANS^- and NPN may disturb the original membrane structure. If these influences are judged by the alterations in T_t due to the presence of the dyes, we arrive at the following conclusion: ANS^- in concentrations below $2\cdot10^{-4}$ M does not cause detectable changes. NPN if present in concentrations beyond $2\cdot10^{-5}$ M (for $c_L=5\cdot10^{-5}$ M) causes a gradual decrease in T_t or a fluidization of the lipid matrix. Nevertheless, our values of ρ appear trustworthy because (a) the effect of NPN on the lipid organization is expected to be the same for the membranes and the lipid dispersions (standard), and because (b) the lowering of T_t for high NPN concentrations does not affect the linear relationship between $1/\Delta I$ and $1/c_{NPN}$ as seen in Fig. 9.

Summarizing, it appears that the value of ρ is correct within the given limits of $\pm5\%$; in contrast, the value of μ is subject to systematic errors (points 4, 5, 6). However, since all these effects tend to increase the apparent value of μ we may state that the given value of μ ($=53\%$) represents an upper limit.

DISCUSSION

The experiments yield estimates for two membrane parameters; (a) A fraction $\rho=80\pm6\%$ of the membrane lipids takes part in the lipid phase transition. These lipid molecules must be organized in a form which permits direct and cooperative interaction between the hydrocarbon chains [(dis)continuous mono- or bilayers].

(b) A fraction $\mu = 53 \pm 5\%$ of these lipids (or 42.5% of the total membrane lipids) is directly accessible to ANS^- molecules.

Our first value (ρ) can be compared with similar estimates in the literature. Steim *et al.*[1] compared the transition enthalpies of membranes and isolated lipids of *Mycoplasma* and arrived at a value of 75% for the lipid fraction ρ. Using the same approach, Reinert and Steim[2] estimated ρ to be $90 \pm 10\%$. This value was interpreted as the portion of the lipids in bilayer form, a view criticized by Chapman and Urbina[47]. Applying X-ray diffraction to *Mycoplasma* membranes, Engelman[4] estimated that at least 80% of the lipid chain diffraction in the wide-angle region is involved in the lipid phase transition. More recently Engelman[48] reported that $\rho = 70$–100% where the lower limit of 70% was considered as a firm one: "The uncertainty in these X-ray measurements arises from the difficulty of establishing a baseline against which to measure the band". Values of 80% and 84% for the fraction of lipids in a "fluid" state have been reported by Metcalfe *et al.*[49] and McConnell *et al.*[50] for membranes of *Mycoplasma* and rabbit muscle sarcoplasmic reticulum, respectively. These results were obtained by comparing the solubility of the spin label TEMPO (2,2,6,6-tetramethylpiperidine-1-oxyl) in membranes and in lipid standards. In summary, a fraction of the membrane lipids between 70–100% has been estimated to be in a bilayer (and/or monolayer) state for three different systems using different assays. In contrast, values for μ are not available in the literature.

The values of ρ ($=80\%$) and μ ($=53\%$) can be used as a starting point for quantitative model considerations of the membrane structure. The main features of the model to be discussed (Davson–Danielli–Robertson–Benson–Singer membrane model) are illustrated in Fig. 12a*. The membrane matrix is shown as a lipid bilayer (fraction ρ of the total lipids) into which individual integral proteins (P_i) penetrate. Part of the lipids is assumed to be closely associated with integral proteins ("non-bilayer" fraction $\rho' = 1 - \rho$). The average number of lipid molecules coupled to one protein molecule, P_i, is denoted in the following by ξ. These molecules are located within the cross-hatched areas in Fig. 12. Layers of peripheral proteins (P_i) are assumed to cover a fraction $(1-\mu)$ of the bilayer surface on both sides of the membrane. Since our data do not contain information about possible asymmetries in the membrane structure a symmetrical membrane model is considered in the following.

Membrane matrix

An area F ($=1$ cm^2) of the membrane matrix may be divided into three parts (*cf.* Fig. 12b):

$$F = N'_L f'_L + N_L f_L + N_{P_i} f_{P_i} \tag{1}$$

where

$$N'_L = \rho' \times N_L^{tot} \tag{2}$$

denotes the number of lipid molecules in non-bilayer state, and

$$N_L = \rho \times N_L^{tot} \tag{3}$$

* We do not intend here to discuss the pro's and contra's of this model. Several review articles are available in which the different arguments are discussed in great detail: Stoeckenius and Engelman[20]; Singer[22]; Hendler[21]; Gitler[60]. Rather our intention is to estimate the parameters of the model in Fig. 12a from our experiments.

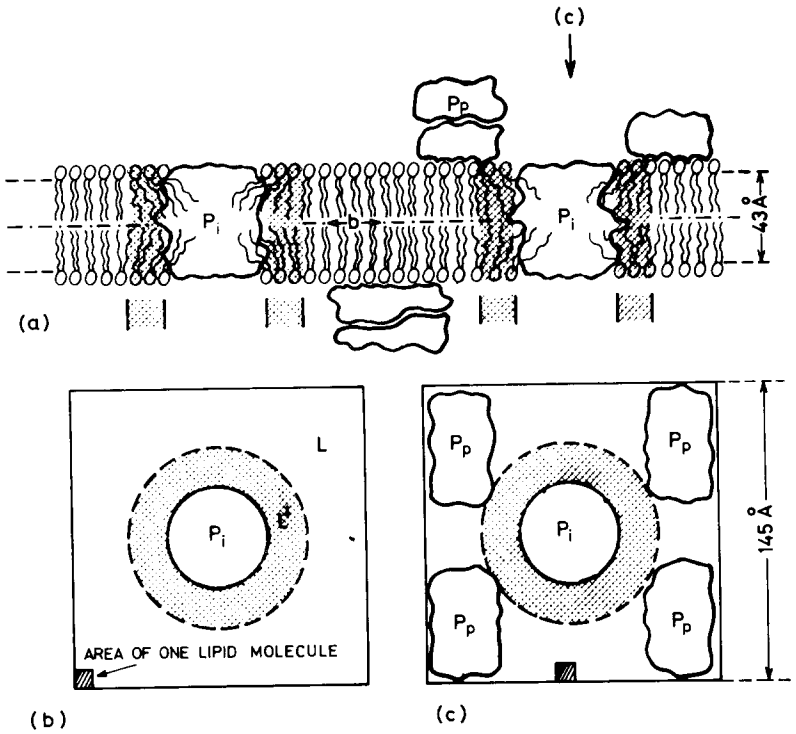

Fig. 12. Davson–Danielli–Robertson–Benson–Singer membrane model reflecting the following set of parameters: $\rho' = 0.20$; $\xi = 125$ and $\mu = 0.53$; see text. (a) Cross section perpendicular to the plane of the membrane. The core of the membrane is shown as an interrupted lipid bilayer through which proteins (P_I) penetrate. These proteins are surrounded by lipids in non-bilayer state (cross-hatched halo) amounting to $\rho' = 20\%$ of the total membrane lipids. Other proteins (P_P) are attached to the membrane surface covering a fraction $\mu = 53\%$ of the lipid bilayer. (b) Cross-section parallel to the plane of the membrane as indicated in Fig. (a). (c) Top view of the membrane as indicated in Fig. (a). Figs (b) and (c) show "unit areas" containing one integral protein and the average number of lipid molecules in its neighborhood. For the above values $\rho' = 0.20$ and $\xi = 125$ this area contains 312 lipid molecules per half plane (*cf.* Table II); 63 of these molecules are in a non-bilayer state around P_I. The molecular areas are assumed as $f_L = 60$ Å^2 for the lipids and $f_{PI} = 2000$ Å^2 for the protein P_I. Then the "unit area" amounts to $(2000 + 312 \times 60) \approx 20\ 700$ Å^2. Actually a lipid bilayer (for $T \gg T_t$) is a highly fluid structure in which a certain lattice point is occupied by the same lipid molecule for not more than about 10^{-7} s (ref. 38).

denotes the number of lipid molecules in bilayer state. N_L^{tot} is the total number of lipid molecules and N_{P_I} the number of integral proteins per cm^2 of the membrane area. In the following we use the convention that N_L, N'_L and N_L^{tot} refer to only half of the membrane matrix (monolayer). In Eqn 1 the symbols f_L, f'_L and f_{PI} denote the molecular areas of the respective lipid and protein molecules.

Denoting the average number of lipid molecules coupled to one protein molecule by the parameter ξ we may write

$$N'_L = \frac{\xi}{2} N_{P_I} \tag{4}$$

Together with Eqn 2 this yields

$$N_{P_i} = 2\frac{\rho'}{\xi}N_L^{tot} \tag{5}$$

Thus for a given fraction, ρ', of "perturbed" lipid molecules the number of integral proteins is large for small values of ξ, and *vice versa*. This is simply a consequence of the assumption that all of the perturbed molecules be associated with integral proteins and that every protein is surrounded by an average number, ξ, of perturbed lipid molecules.

Combining Eqns 1 to 4 and approximating $f_L \approx f_L'$ yields for the number N_{P_i} of integral membrane proteins

$$N_{P_i} = \frac{F}{f_{P_i} + f_L\xi(\rho/\rho' + 1)/2} \tag{6}$$

In Tables I and II values of N_{P_i} and (N_L^{tot}/N_{P_i}) are listed for several combinations of ξ and ρ'. According to our measurements $\rho' = 0.20$. A range between 10 and 200 was

TABLE I

NUMBER OF INTEGRAL PROTEINS N_{P_i} PER cm² OF THE MEMBRANE (IN UNITS OF 10^{11}) CALCULATED FROM EQN 6 FOR SEVERAL COMBINATIONS OF ξ AND ρ' (SEE TEXT)

The cross-sectional area of one protein molecule was assumed as $f_{P_i} = 1500$ Å² and $f_{P_i} = 2500$ Å² (values in parentheses).

ξ	$\rho' = 0.10$	$\rho' = 0.15$	$\rho' = 0.20$	$\rho' = 0.25$
10	22 (18)	28.6 (22)	33 (25)	37 (27)
25	11 (10)	15.4 (13)	19 (16)	22 (18)
50	6.1 (5.7)	8.7 (8)	11 (10)	13 (12)
75	4.2 (4)	6.1 (5.7)	7.9 (7.3)	9.5 (8.7)
100	3.2 (3.1)	4.6 (4.4)	6.1 (5.7)	7.4 (7)
125	2.6 (2.5)	3.8 (3.6)	4.9 (4.7)	6.1 (5.7)
150	2.1 (2.1)	3.2 (3.1)	4.2 (4.0)	5.1 (4.9)
200	1.6 (1.6)	2.4 (2.3)	3.2 (3.1)	3.9 (3.8)

TABLE II

RATIO N_L^{tot}/N_{P_i} OF THE NUMBER OF LIPID MOLECULES PER HALF PLANE OF THE MEMBRANE (N_L^{tot}) TO THE NUMBER OF INTEGRAL PROTEINS N_{P_i}, CALCULATED FROM EQN 5 FOR SEVERAL COMBINATIONS OF ξ AND ρ'

ξ	$\rho' = 0.10$	$\rho' = 0.15$	$\rho' = 0.20$	$\rho' = 0.25$
10	50	33.3	24	20
25	125	83.5	62.5	50
50	250	167	125	100
75	375	250	187	150
100	500	333	250	200
125	625	417	312	250
150	750	500	375	300
200	1000	670	500	400

chosen for ξ. The values of N_{P_i} (Table I) were calculated for $f_{P_i} = 1500$ (2500) Å^2 and $f_L = 60$ Å^2 [Chapman *et al.*[45]; Levine and Wilkins[18]; Small[51]; Reiss-Husson[52]]. The value $f_{P_i} = 2500$ Å^2 is the approximate cross-sectional area of a globular protein with a molecular weight of 100000 and a radius $r = 30$ Å; $f_{P_i} = 1500$ Å^2 would correspond to a globular protein with a molecular weight of 50000, or to a cylindrical protein molecule of the same weight and a height of 50 Å. The exact choice of f_{P_i} does not greatly alter the numerical results because the term f_{P_i} is small compared to the second term in the denominator of Eqn 6 for the interesting range $\xi \geq 50$. If, for example, 50 lipid molecules were coupled to each protein then one integral protein would be surrounded on average by 250 lipid molecules ($= 2\, N_L^{tot}$), (*cf.* Table II, $\xi = 50$, $\rho' = 0.20$).

The internal surface of several plasma membranes has been revealed by freeze–etching electron microscopy (*E. coli*: van Gool and Nanninga[53]; *Mycoplasma laidlawii*: Tillack *et al.*[54]; erythrocytes: Branton[55]; Da Silva and Branton[56]). These pictures show "particles" with a density of $(1–5) \cdot 10^{11}$/cm^2. Interpreting these particles as integral proteins [Meyer and Winkelman[57]; Da Silva and Branton[56]] would mean that on average at least 125 lipid molecules are coupled to each protein molecule (*cf.* Table I, $\rho' = 0.20$). The corresponding membrane area (cross hatched in Fig. 12b) is about twice that of the cross-sectional area of one protein molecule. Thus our analysis allows us to calculate the density of integral proteins, N_{P_i}, from a known value of ρ' and an assumed value for ξ, or alternatively, and more interestingly, we may estimate the average number, ξ, of lipid molecules coupled to one integral protein from a known value of N_{P_i}.

If integral proteins penetrate the membrane matrix as assumed in Fig. 12a then the lipid layer accounts for only a fraction q of the total membrane area. Using Eqn 5 the fraction q may be expressed as

$$q = \frac{N_L^{tot} f_L}{N_L^{tot} f_L + N_{P_i} f_{P_i}} = \frac{1}{1 + 2\frac{\rho'}{\xi}\frac{f_{P_i}}{f_L}} \tag{7}$$

Taking $f_L = 60$ Å^2, $\rho' = 0.2$ and $\xi = 125$ this expression yields $q = 0.93$ for $f_{P_i} = 1500$ Å^2 and $q = 0.88$ for $f_{P_i} = 2500$ Å^2. This means that the integral proteins account for about 10% of the membrane matrix. Recently Engelman[58] estimated the value of q for human red blood cells as $q = 0.8–0.9$.

Membrane surface

Two experimental parameters are available to characterize the membrane surface:

(1) The fraction μ of the lipid bilayer that is in contact with the water. Using the symbol, F^{free}, for the "free" area on both sides of the membrane (1 cm^2) we may write

$$\mu = F^{free}/2N_L f_L \tag{8}$$

In the following we assume that peripheral proteins are attached only to the lipids in bilayer form.

(2) The weight ratio ϕ of the membrane proteins to the membrane lipids. ϕ may be expressed as

$$\phi = \frac{N_{P_i} M_{P_i} + N_{P_p} M_{P_p}}{2N_L^{tot} M_L} \tag{9}$$

Here N_{P_i} denotes the number of integral proteins per cm^2 of the membrane; N_{P_p} is the number of peripheral proteins on either side of the membrane; M_{P_i} and M_{P_p} are the respective molecular weights and M_L (=777) is the molecular weight of the lipids. In the present case $\phi=2$.

Since it is not known if the peripheral proteins make up exactly one layer we introduce a stacking parameter, ζ, denoting the fraction of peripheral proteins that is in direct contact with the lipid polar groups. Thus the free area, F^{free}, of the lipid bilayer is given by

$$F^{free} = 2N_L f_L - \zeta N_{P_p} f_{P_p} \tag{10}$$

where f_{P_p} denotes the average area of the lipid bilayer occupied by one peripheral protein layered directly on the lipids. Using Eqn 8 for μ yields

$$N_{P_p} = \frac{2N_L f_L(1-\mu)}{f_{P_p}} \frac{1}{\zeta} \tag{11}$$

Combining Eqns 11, 9, 5 and 3 leads to an expression for f_{P_p}:

$$f_{P_p} = \frac{(1-\mu)\rho}{(\phi M_L/M_{P_i} - \rho'/\xi)} \left(\frac{M_{P_p}}{M_{P_i}}\right) \frac{f_L}{\zeta} \approx \frac{(1-\mu)\rho}{\phi} \frac{M_{P_p}}{M_L} \frac{f_L}{\zeta} \tag{12}$$

The latter approximation is valid for $\xi \geq 25$ and $M_{P_p} = M_{P_i}$. Using the experimental results $\mu=0.53$, $\phi=2$, $\rho=0.80$, $M_L=777$ and assuming $M_{P_p}=50000$ yields

$$f_{P_p} \approx 12 f_L/\zeta \tag{13}$$

For $\zeta=1$ the peripheral proteins would make up exactly one surface layer. In this case the area available for one protein molecule is equivalent to the area of 12 lipid molecules ($12 \cdot 60$ Å$^2 = 720$ Å^2). Values of f_{P_p} between $(25\text{–}40) \times f_L$ would be expected for proteins with a molecular weight between 50000 and 100000. The assumption $\zeta=0.5$, would correspond to a "double layer" of proteins; in this case $f_{P_p} \approx 24 f_L$. Alternatively, a value of $f_{P_p} = 24 \times f_L$ is obtained for $M_{P_p}=100000$ and $\zeta=1$. In summary, it appears that some of the surface proteins are stacked.

From the foregoing it is easy to estimate the weight ratio, *wr*, of the integral to the total membrane proteins $[w_P = N_{P_i} M_{P_i}/(N_{P_i} M_{P_i} + N_{P_p} M_{P_p})]$. Using the expressions 5 and 9 with $\phi=2$ and approximating $M_{P_i} = M_{P_p}$ one obtains $w_P = M_P \rho'/2M_L \xi$. For $\rho'=0.2$, $\xi=125$, $M_L=777$, $M_P=50000$ (100000) one calculates $w_P=5\text{–}10\%$.

The results of our discussion are summarized in Fig. 12 in a drawing to scale of the considered membrane model. Fig. 12a shows a cross-section perpendicular to the plane of the membrane; Figs 12b and 12c depict "unit areas" of the membrane containing one integral protein and the average number of lipid molecules around it. The areas occupied by the different membrane constituents (peripheral and

integral proteins, lipids in bilayer and non-bilayer state) are drawn according to the following set of parameters: $\rho' = 0.2$ (fraction of the lipids in non-bilayer state); $\mu = 0.53$ (fraction of the lipid bilayer not occupied by peripheral proteins); and $\xi = 125$ (number of lipid molecules associated with one integral protein).

For these parameters we read from Table II $N_L^{tot}/N_{P_i} = 312$, which means that on the average one integral protein ($f_P \approx 2000$ Å^2) is surrounded by 312 lipid molecules ($f_L \approx 60$ Å^2) in one half plane of the membrane. An average number of $\xi = 125$ lipid molecules is coupled to each integral protein corresponding to a perturbed area (or halo) of about $\xi/2 \times f_L \approx 62 \times 60 = 3800$ Å^2 (cross hatched area in Fig. 12). The unit area shown in Figs 12b and 12c amounts to $(312 \times 60 + 2000 \approx) 21 \cdot 10^3$ Å^2.

Finally we consider the case that the integral proteins do not span the entire membrane thickness as assumed in Fig. 12a, but instead penetrate only half into the lipid bilayer (proteins embedded in either monolayer). It is easily checked that Eqn 12 remains unaltered. However, Eqn 6 reads now

$$N_{P_i}^{tot} = \frac{2F}{f_{P_i} + \xi f_L (1 + \rho/\rho')}$$

where $N_{P_i}^{tot}$ denotes the number of integral proteins in an area F of the membrane. For the interesting case $f_{P_i} \ll \xi f_L (1 + \rho/\rho')$ we obtain the same results as from Eqn 6. More precisely, if we determine the lower limit of ξ using the value $5 \cdot 10^{11}$/cm^2 for the number of integral proteins per cm^2 of the membrane we obtain $\xi = 132$ instead of $\xi = 125$. Thus the results for ξ and f_{P_p} (Eqn 13) are virtually the same as before. However, since now the perturbed lipid molecules are located virtually in one half of the lipid matrix (monolayer) the area of the halo (cross-hatched area in Fig. 12b) is about twice that shown in Fig. 12b.

At present the fraction of integral proteins that span the entire membrane or only half of it, is not known. Therefore we can only conclude that the cross-hatched area in Fig. 12b (drawn on the basis $\xi = 125$) represents a lower limit for the area of perturbed molecules coupled to one integral membrane protein.

Finally we would like to emphasize again that our results are averages over both sides of the membrane and over a large variety of membrane proteins.

ACKNOWLEDGEMENTS

This work has benefited from discussions with Prof. W. Stoeckenius. We are indebted to Dr P. Zingsheim for many critical comments. The assistance of Miss S. Schröder is gratefully acknowledged. This work was supported by the Deutsche Forschungsgemeinschaft through SFB 74 and 33.

APPENDIX: FLUORESCENCE CHANGE ΔI AT THE PHASE TRANSITION

The fluorescence intensity I^{tot} of fluorescence probes such as ANS^- or NPN in dispersions of lipids (or membranes) contains contributions from the free (c_D^0) and bound (c_D^*) probe molecules:

$$I^{tot}(\lambda_{exc}, \lambda_{em}) = Q^* c_D^* + Q^0 c_D^0 \tag{A1}$$

Here I^{tot} is the fluorescence intensity corrected for inner filter and light scattering

effects. λ_{exc} and λ_{em} denote the wavelengths of excitation and emission, and Q^* and and Q^O denote the quantum yields of the adsorbed and free dye molecules, respectively. In writing Eqn A1 we have assumed that only one type of binding site exists.

Subtracting the fluorescence intensity of the free dye, yields

$$I = Q^* c_D^* \tag{A2}$$

In the further discussion we take the binding of ANS^- to lipid dispersions (or membranes) as example. Provided the surface charge of the membranes is low and/or the ionic strength is high (≥ 0.05) the binding of ANS^- is governed to a good approximation by a simple Langmuir type of adsorption law which is described by the scheme

$$D + B \underset{k_d}{\overset{k_b}{\rightleftharpoons}} (DB) \tag{A3}$$

Here we have used the symbols D for dye (concentration c_D), B for binding site (concentration c_B) and $(DB) = B^* = D^*$ for occupied binding sites or bound dye molecules; ($c_D^{tot} = c_D^* + c_D^O$; and $c_B^{tot} = c_B^* + c_B^O$). $K_d = k_d/k_b$ is the dissociation equilibrium constant.

Applying the law of mass action to the scheme A3 yields

$$\frac{1}{c_D^*} = \frac{1}{c_B^{tot}} + \frac{K_d}{c_B^{tot}(c_D^{tot} - c_D^*)} \tag{A4}$$

The number of binding sites c_B^{tot} can be written as $c_B^{tot} = nc_L$ where c_L denotes the lipid concentration.

Our experiments were performed under conditions where $c_D^{tot} \gg c_D^*$; Thus

$$\frac{1}{c_D^*} = \frac{1}{nc_L} + \frac{K_d}{nc_L c_D^{tot}} \tag{A5}$$

For highly charged membranes and/or low ionic strength K_d is a function of c_D^* due to the increasing surface charge in the course of the adsorption of the negatively charged ANS^-. However, at high ionic strength, as in our experiments, K_d is a constant.

Then the fluorescence intensity I of the adsorbed dye molecules is given by

$$I = \frac{Q^* nc_L}{1 + K_d/c_D^{tot}} \tag{A6}$$

As seen in Figs 2b and 4b straight lines are obtained in the temperature ranges below and above the phase transition if $\log I$ is plotted against $1/T$. The fluorescence change ΔI at the phase transition is defined as the vertical distance $\Delta I = I_2 - I_1$ between the two extrapolated straight lines at a temperature, T_t, where the curve $I(T)$ bisects the vertical difference (numerus) between the two straight lines. If Eqs A5 and A6 are obeyed in the temperature ranges above and below the phase transition then, also, the (extrapolated) values $I_2(T)$ and $I_1(T)$ may be calculated according to Eqn A6 whereby different sets of parameters (n_2, Q_2^*, K_{d2}) and (n_1, Q_1^*, K_{d1}) are valid for States 1 and 2.

Then the dependence of ΔI on the dye concentration c_D^{tot} is given by

$$\Delta I = I_2 - I_1 = Q_2^* \; c_{D2}^* - Q_1^* \; c_{D1}^*$$

$$= \frac{Q_2^* \; n_2 c_L}{1 + K_{d2}/c_D^{tot}} - \frac{Q_1^* \; n_1 c_L}{1 + K_{d1}/c_D^{tot}} \tag{A7}$$

The limiting value $(\Delta I)_{lim}$ for $c_D^{tot} \to \infty$ is

$$(\Delta I)_{lim} = c_L(Q_2^* \; n_2 - Q_1^* \; n_1) \tag{A8}$$

where c_L denotes the lipid fraction which (a) participates in the phase transition and (b) serves as adsorption matrix for the fluorescent dye. For ANS^- in dispersions of dipalmitoyllecithin the values of Q^*, n and K_d have been determined for the states below and above the phase transition[36]. The results indicate that $(\Delta I)_{lim}$ is determined virtually by differences in n_2 and n_1. In contrast, for phosphatidylethanolamines the values of Q_1^* and Q_2^* are different. For the lipids extracted from the *E. coli* membranes (predominantly phosphatidylethanolamines) one determines $Q = 0.015$ at 25 °C and $Q = 0.025$ at 45 °C.

Eqn A8 shows that a comparison of the $(\Delta I)_{lim}$ values of two systems (with known and unknown c_L) can be used to determine the unknown lipid fraction. An easy determination of c_L is possible only if the quantity $(Q_2^* n_2 - Q_1^* n_1)$ is the same for the two systems which means that the lipid matrices of the two systems should be identical.

According to Eqn A7 a reciprocal plot of $1/\Delta I$ *versus* $1/c_D^{tot}$ is expected to yield a straight line if $\Delta K_d = K_{d2} - K_{d1}$ is small compared to c_D^{tot}. For this case (writing $K_{d1} \approx K_{d2} \approx K_d$) we obtain

$$\frac{1}{\Delta I} = \frac{1}{c_L(Q_2^* \; n_2 - Q_1^* \; n_1)} \left[1 + \frac{K_d}{c_D^{tot}} \right] \tag{A9}$$

If we compare two systems with identical values of $(Q_2^* n_2 - Q_1^* n_1)$ but different K_d the slopes in the $1/\Delta I$ *versus* $1/c_D^{tot}$ plot are expected to be different. Nevertheless the intercept with the zero ordinate can be used as a measure of c_L.

REFERENCES

1 Steim, J. M., Tourtelotte, M. E., Reinert, J. C., McElhaney, R. N. and Rader, R. L. (1969) *Proc. Natl. Acad. Sci. U.S.* 63, 104–109
2 Reinert, J. C. and Steim, J. M. (1970) *Science* 168, 1580–1582
3 Engelman, D. M. (1970) *J. Mol. Biol.* 47, 115–117
4 Engelman, D. M. (1971) *J. Mol. Biol.* 58, 153–165
5 Wilson, G., Rose, S. P. and Fox, C. F. (1970) *Biochem. Biophys. Res. Commun.* 38, 617–623
6 Overath, P., Schairer, H. U. and Stoffel, W. (1970) *Proc. Natl. Acad. Sci. U.S.* 64, 606–612
7 Overath, P. and Träuble, H. (1973) *Biochemistry*, in the press
8 Blazyk, J. F. and Steim, J. M. (1972) *Biochim. Biophys. Acta* 266, 737–741
9 Nielsen, J. R. and Hathaway, C. E. (1963) *J. Mol. Spectrosc.* 10, 366–377
10 Messerly, J. F., Guthrie, G. B., Tod, S. S. and Finke, H. L. (1967) *J. Chem. Eng. Data* 12, 338
11 McClure, D. W. (1968) *J. Chem. Phys.* 49, 1830–1839

12 Blasenbrey, S. and Pechhold, W. (1967) *Rheol. Acta* 6, 174–185
13 Sackmann, E. and Träuble, H. (1972) *J. Am. Chem. Soc.* 94, 4482–4491
14 Sackmann, E. and Träuble, H. (1972) *J. Am. Chem. Soc.* 94, 4492–4498
15 Wilkins, M. H. F., Blaurock, A. E. and Engelman, D. M. (1971) *Nat. New Biol.* 230, 72–76
16 Caspar, D. L. D. and Kirschner, D. A. (1971) *Nat. New Biol.* 231, 46–52
17 Blaurock, A. E. (1972) *Chem. Phys. Lipids* 8, 285–291
18 Levine, Y. K. and Wilkins, M. H. F. (1971) *Nat. New Biol.* 230, 69–72
19 Levine, Y. K. (1972) in *Progr. Biophys. and Mol. Biol.* (Butler, J. A. V. and Noble, D., eds), Vol. 24, pp. 1–74, Pergamon Press, Oxford
20 Stoeckenius, W. and Engelman, D. M. (1969) *J. Cell. Biol.* 42, 613–646
21 Hendler, R. W. (1971) *Physiol. Rev.* 51, 66–97
22 Singer, S. J. (1971) in *Structure and Function of Biological Membranes* (Rothfield, L. I., ed.), pp. 145–222, Academic Press, New York
23 Singer, S. J. and Nicolson, G. L. (1972) *Science* 175, 720–731
24 Razin, S. (1972) *Biochim. Biophys. Acta* 265, 241–296
25 Rubalcava, B., Martinez-Rojas, D. and Gitler, C. (1969) *Biochemistry* 8, 2742–2747
26 Brocklehurst, J. R., Freedman, R. B., Hancock, D. J. and Radda, G. K. (1970) *Biochem. J.* 116, 721–731
27 Vanderkooi, J. and Martonosi, A. (1969) *Arch. Biochem. Biophys.* 133, 153–163
28 Radda, G. K. (1971) *Curr. Topics Bioenerg.* 4, 81–126
29 Radda, G. K. (1971) *Biochem. J.* 122, 385–396
30 Radda, G. K. and Vanderkooi, J. (1972) *Biochim. Biophys. Acta* 265, 509–549
31 Stryer, L. (1965) *J. Mol. Biol.* 13, 482–495
32 Gulik-Krzwicki, F., Schechter, E., Iwatsubo, M., Ranck, J. L. and Luzzati, V. (1970) *Biochim. Biophys. Acta* 219, 1–10
33 Lesslauer, W., Cain, J. and Blasie, J. K. (1971) *Biochim. Biophys, Acta* 241, 547–566
34 Zingsheim, H. and Haydon, D. A. (1973) *Biochim. Biophys. Acta* 298, 755–768
35 Gomperts, B., Lantelme, F. and Stock, R. (1970) *J. Membrane Biol.* 3, 241–266
36 Träuble, H. (1971) *Naturwissenschaften* 58, 277–284
37 Colley, C. M. and Metcalfe, J. C. (1972) *FEBS Lett.* 24, 241–246
38 Träuble, H. and Sackmann, E. (1972) *J. Am. Chem. Soc.* 94, 4499–4510
39 Träuble, H. (1972) in *Biomembranes* (Kreutzer, F. and Slegers, J. F. G., eds), Vol. 3, pp. 197–227, Plenum Press
40 Devaux, P. and McConnell, H. M. (1972) *J. Am. Chem. Soc.* 94, 4475–4481
41 Kaback, H. R. (1971) in *Methods Enzymol.* (Jacoby, W., ed.), Vol. XXII, pp. 99–120, Academic Press, New York
42 Ames, G. F., (1968) *J. Bacteriol.* 95, 833.
43 Fortes, P. A. G. (1972) Ph. D. Thesis, University of Pennsylvania.
44 Bergelson, L. D., Barsukov, L. I., Dubrovnia, N. I. and Bystrov, V. F. (1970) *Dokl. Biophys.* 194, 703
45 Chapman, D., Williams, R. M. and Ladbrooke, B. D. (1967) *Chem. Phys. Lipids* 1, 445–475
46 Kamat, V. B., Wyatt, A. J. and Davies, M. A. F. (1972) *Chem. Phys. Lipids* 8, 341–346
47 Chapman, D. and Urbina, J., (1971) *FEBS Lett.* 12, 169–172
48 Engelman, D. M. (1972) *Chem. Phys. Lipids* 8, 298–302
49 Metcalfe, J. C. Birdsall, N. J. M. and Lee, A. G. (1972) *FEBS Lett.* 21, 335–340
50 McConnell, H. M., Wright, K. L. and McFarland, B. G. (1972) *Biochem. Biophys. Res. Commun.* 47, 273–281
51 Small, D. M. (1967) *J. Lipid Res.* 8, 551
52 Reiss-Husson, P. (1967) *J. Mol. Biol.* 25, 363–382
53 Van Gool, A. P. and Nanninga, N. (1971) *J. Bacteriol.* 168, 474
54 Tillack, T. W. Carter, R. and Razin, S. (1970) *Biochim. Biophys. Acta* 219, 123–130
55 Branton, D. (1971) *Phil. Trans. Soc. London.* B 261, 133
56 Da Silva, P. P. and Branton, D. (1972) *Chem. Phys. Lipids* 8, 265–278
57 Meyer, H. W. and Winkelmann, H. (1969) *Protoplasma* 68, 253–270
58 Engelman, D. M. (1969) *Nature* 223, 1279–1280
59 Turner, D. G. and Brand, L. (1968) *Biochemistry* 7, 3381–3390
60 Gitler, C. (1972) *Annu. Rev. Biophys. Bioeng.* 1, 51–92